Current Biology *16*, 2111–2122, November 7, 2006 DOI 10.1016/j.cub.2006.09.030

Article

Spindle Oscillations during Asymmetric Cell Division Require a Threshold Number of Active Cortical Force Generators

Jacques Pecreaux,[1,5] Jens-Christian Röper,[1,2,5] Karsten Kruse,[3,4] Frank Jülicher,[3] Anthony A. Hyman,[1] Stephan W. Grill,[1,3,*] and Jonathon Howard[1,*]

[1] Max-Planck Institute for Molecular Cell Biology and Genetics
Pfotenhauerstrasse 108
01307 Dresden
Germany

[2] Freie Universität Berlin
Fachbereich Biologie, Chemie, Pharmazie
Takustrasse 3
14195 Berlin
Germany

[3] Max-Planck Institute for the Physics of Complex Systems
Nötnitzerstrasse 38
01187 Dresden
Germany

Summary

Background: Asymmetric division of the *C. elegans* zygote is due to the posterior-directed movement of the mitotic spindle during metaphase and anaphase. During this movement along the anterior-posterior axis, the spindle oscillates transversely. These motions are thought to be driven by a force-generating complex—possibly containing the motor protein cytoplasmic dynein—that is located at the cell cortex and pulls on microtubules growing out from the spindle poles. A theoretical analysis indicates that the oscillations might arise from mechanical coordination of the force-generating motors, and this coordination is mediated by the load dependence of the motors' detachment from the microtubules. The model predicts that the motor activity must exceed a threshold for oscillations to occur.

Results: We have tested the existence of a threshold by using RNA interference to gradually reduce the levels of dynein light intermediate chain as well as GPR-1 and GPR-2 that are involved in the G protein-mediated regulation of the force generators. We found an abrupt cessation of oscillations as expected if the motor activity dropped below a threshold. Furthermore, we can account for the complex choreography of the mitotic spindle—the precise temporal coordination of the build-up and die-down of the transverse oscillations with the posterior displacement—by a gradual increase in the processivity of a single type of motor machinery during metaphase and anaphase.

Conclusions: The agreement between our results and modeling suggests that the force generators themselves have the intrinsic capability of generating oscillations when opposing forces exceed a threshold.

Introduction

Asymmetric cell divisions are common during embryogenesis and neurogenesis, where they contribute to the generation of cell-fate diversity [1, 2]. During such divisions, the mitotic spindle is off-center at the end of anaphase; when the cleavage furrow bisects the spindle [3], it therefore generates two daughter cells of unequal size. An example is the division of the one-cell embryo of the nematode *C. elegans*. At the beginning of metaphase, the mitotic spindle is positioned in the center of the cell, aligned along the anterior-posterior (AP) axis, which coincides with the long axis of the cell. During metaphase and anaphase, the spindle elongates and its center moves toward the posterior cortex, resulting in an off-center spindle. The asymmetry is determined by the cell's polarity, which is established after fertilization [4] through the activity of the *par* genes [5, 6]. The PAR proteins and associated components localize to the anterior or posterior half of the cell cortex [7] and lead to the preferential localization of the G protein regulators GPR-1 and GPR-2 to the posterior cortex [8–10]. The association of GPR-1 and GPR-2 with Gα [8, 11, 12] is thought to activate force generators located at the cortex. The force generators pull on the astral microtubules emanating from the spindle poles, with a larger force acting on the posterior pole than on the anterior one [13]. The forces increase during metaphase and anaphase [14], and their increasing imbalance displaces the spindle into the posterior half of the embryo.

During its movement into the posterior half of the embryo, the mitotic spindle of the *C. elegans* zygote begins to oscillate transversely as the two spindle poles move perpendicular to the AP axis in a sinusoidal manner ([15, 16], Figure 1). The displacement of the posterior pole is larger than that of the anterior pole, and the oscillations of the two poles are out of phase (Figure 1C); the spindle therefore appears to rotate, or rock, about a point closer to the anterior pole. The amplitude of the oscillations steadily builds up, reaches a peak when the spindle reaches its most-posterior position, and then dies down. The function of the oscillations is unknown, although oscillations are often associated with asymmetric cell divisions [17, 18].

Several observations suggest that the oscillations are driven by the same regulatory or motor mechanisms that drive the posterior displacement. First, interfering with the G protein signaling pathway that controls posterior spindle displacement leads to loss of oscillations [8–12]. Second, because the poles continue to oscillate transversely even after the spindle has been bisected with a laser [13], the oscillations, like the posterior displacement itself [14], are generated by forces originating

*Correspondence: grill@mpi-cbg.de (S.W.G.), howard@mpi-cbg.de (J.H.)

[4] Present address: Theoretische Physik, Universität des Saarlandes, 66041 Saarbrücken, Germany.

[5] These authors contributed equally to this work and are listed alphabetically.

from outside of the spindle (i.e., at the cortex). And third, analysis of the radial movement of fragments after disintegration of the spindle poles with a laser indicates that force generators with similar mechanical properties are broadly distributed on the cortex [19]. Such broadly distributed force generators could then mediate both longitudinal displacement and transverse oscillations, although it is puzzling how one type of force generator could drive such very different motions. If the same force generators are indeed responsible for both the posterior displacement and the oscillations, then study of the latter may shed light on the former.

The motor protein cytoplasmic dynein is a good candidate for being a component of the cortical force-generator complex. First, dynein is located at the cortex [20]. Second, oscillations are absent in temperature-sensitive dynein mutants, even at the permissive temperature [21]. Third, dynein has the right polarity to pull on astral microtubules (it is a minus-end-directed motor). And fourth, dynein, in conjunction with its receptor, the dynactin complex, has been implicated in spindle movements in the two-cell embryo [20, 22], in budding yeast [23] and in epithelial cells [24]; in centrosome shape changes in the one-cell *C. elegans* embryo [25]; and in centrosome movements in interphase cells [26–28]. However, the precise role of dynein in spindle movements is still unresolved. This is partly due to the fact that dynein and dynactin are required for spindle formation [20, 22, 29], making molecular dissection of the subsequent movement of the spindle difficult [21]. In addition, because free energy for microtubule depolymerization is already available from the GTPase activity of tubulin [30, 31], a motor protein such as dynein is not necessary for force generation; dynein could therefore mainly play an adaptor or regulatory role, dynamically linking depolymerizing microtubules to the cell cortex. The spatial relationship between the force-generator complex and the microtubules is also unclear. An attractive model is that the complex binds to the end of a microtubule after it reaches the cortex, triggers depolymerization, and continues to hold on to the shrinking end (the complex would be a depolymerase), but alternatively it could bind to the side of the microtubule and walk along it, causing the microtubule to bend at the cortex. Finally, the components of the complex, perhaps dynein itself, could even reach the cortex via the plus ends of the growing microtubules [32], so they could be dynamically associated with the cortex.

In this paper, we have addressed the question of how the force generators, irrespective of their precise molecular composition and operation, could give rise to oscillations. Does one need oscillation of a regulatory molecule to alternately switch on the force generators on one side of the embryo and off on the other? Or can force generators produce oscillations on their own? If the oscillations are intrinsic to the force generators, what properties are needed to coordinate them? These questions have recently been investigated theoretically by Grill et al., who showed that a molecular tug-of-war between cortical force generators pulling from opposite sides of the AP axis can lead to oscillations ([33]; and see Box 1). The key idea behind the model is that the rate of detachment of the force generators from microtubules is load dependent. Such load-dependent unbinding has recently been established by single-molecule experiments on the motor protein kinesin [34] and other biomolecules [35]. The role of load dependence is most easily discussed in the case where motor proteins are the force generators, although the principle is the same whenever there is load-dependent detachment from a depolymerizing microtubule. The load dependence causes the motors to change their behavior in response to the forces that other motors are generating, thereby coordinating the force generators on different sides of the embryo. In Box 1, we present a simplified version of the model discussed by Grill et al. and show how load-dependent antagonistic force generators can give rise to a weakly nonlinear oscillator [36] that produces sinusoidal oscillations similar to those seen in the zygote.

The central prediction of the mechanical model is that oscillations only occur when the total activity of the motors exceeds a threshold value, at which point small spontaneous fluctuations become amplified into large sinusoidal oscillations. We have directly tested the existence of such a threshold by using RNA interference to gradually reduce the levels of dynein light intermediate chain as well as GPR-1 and GPR-2, which are involved in the G protein-mediated regulation of the force generators. We found an abrupt cessation of oscillations as expected if the number of active force generators dropped below a threshold. We then asked how the activity of the force generators is regulated. We found that the complex choreography of the mitotic spindle—the precise temporal coordination of the buildup and die-down of the transverse oscillations with the posterior displacement—could be completely accounted for by a gradual increase in the processivity of the force generators during metaphase and anaphase.

Results

Oscillations in Unperturbed Embryos

The mitotic spindle of the one-cell *C. elegans* embryo oscillates transversally as it elongates and moves toward the posterior side of the cell (Figure 1, Movie S1 in the Supplemental Data available online; oscillations observed in 24/24 embryos at 23°C). The oscillations were quantified by fluorescently labeling the anterior and posterior poles with GFP-γ-tubulin (Figure 1A) and tracking their positions over time (Figure 1B). The oscillations built up and died down over 2 to 3 min (Figure 1C). The rising phase could be fit with a single exponential that increased *e*-fold per 45 ± 19 s (mean ± standard deviation [SD], n = 24 embryos, 23°C). The oscillation reached a maximum amplitude of 3.14 ± 0.84 μm (from the AP axis) for the posterior pole and 1.92 ± 0.68 μm for the anterior pole (n = 22). In all embryos, the maximum posterior amplitude was greater than the anterior one. The oscillations then decayed exponentially with a time constant of 21 ± 4 s (n = 22). The onset of the oscillation lagged the onset of spindle displacement by about 1 min, and the oscillation began to die down at about the time that the spindle reached its maximum posterior displacement (Figure 1D). The final displacement of the center of the spindle was 5.0 ± 0.7 μm (n = 22), measured from the center of the embryo toward the posterior (the average initial position was 0.6 ± 1.1 μm from the center).

Box 1. The Antagonistic-Motors Model

The model described here is a simplification of that developed in Grill et al. [B1]. We first describe qualitatively how load-dependent motors give rise to oscillations and then present the equations. The derivation of the equations together with a justification of the choice of parameter values is given in the Supplemental Data. The parameters used in the simulation are listed in the legend to Figure 5.

Consider cortical motors pulling on astral microtubules emanating from the posterior pole (Box 1, Figure 1A).

(1) Suppose that the pole is undergoing transverse oscillations (up and down in Box 1, Figure 1) and that the pole is at the most downward part of its cycle and just beginning to move upward toward the AP axis. At this point in the motion, the speed is zero and we assume that there is a centering process that pulls the pole toward the AP axis. We call this the "centering spring", and we infer its existence from the observation that the spindle is precisely centered on the AP axis prior to spindle oscillations. The molecular basis for this centering spring could be the pushing or pulling of microtubules [B2] that contact the cortex at sites that may be distinct from the cortical force generators. At this time, there are more active motors at the lower cortex than at the upper cortex, and the difference in cortical forces is balanced by the force in the centering spring.

(2) As the upward speed increases, the load on the upper motors decreases. As a result of the load-dependent detachment, the number of attached upper motors increases. If the load dependence is strong enough, the increase in number of attached motors will be large enough to increase the total force generated by all the upper motors even though the force per motor has decreased. This is positive feedback! An analogous process occurs at the lower cortex: The load per motor increases, the number of attached motors decreases, the load per motor increases, and more motors detach. Such catastrophic detachment also constitutes positive feedback. The net result is an increasing upward force that augments the force from the centering spring.

(3) As the pole moves across the AP axis, the centering spring will oppose the pole's further movement toward the upper cortex. However, the upper motors do not respond immediately to this opposing force: They are processive and they only detach after a delay. This delay gives rise to the equivalent of inertia in the system. (Note, however, that all true inertial forces can be neglected and that inertia-like properties result solely from the attachment and detachment kinetics of motors.) As a consequence, the spindle overshoots the AP axis before finally stopping at the most upward part of the cycle.

(4) The cycle then continues in the other direction. If there were no positive feedback, the oscillations would slowly die out as a result

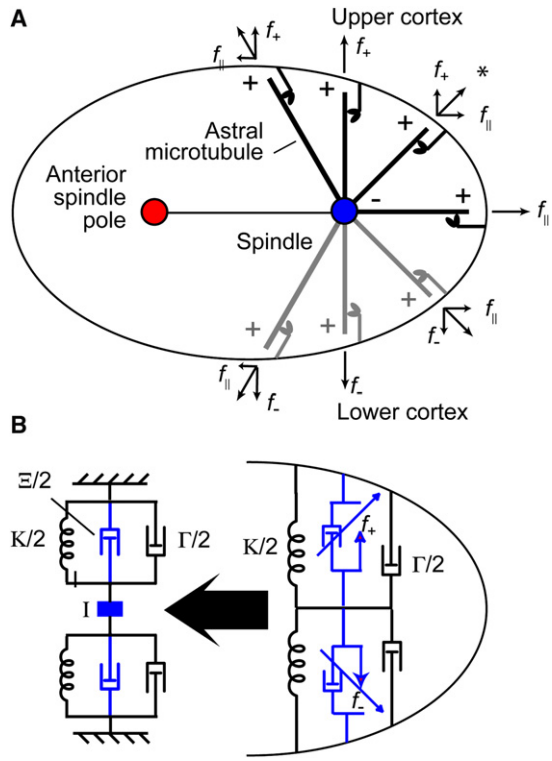

Figure 1. Model of Mechanical Oscillations Driven by a Symmetric Distribution of Cortical Force Generators

(A) Subset of astral microtubules emanating from the posterior spindle pole interacts with motor proteins attached to the cell cortex. Not shown are other posterior microtubules (growing, shrinking, or interacting at other sites on the cortex), anterior astral microtubules, and the spindle microtubules. The motors are part of a force-generating complex that pulls on the microtubules, creating tension that pulls the spindle pole toward the cortex as the microtubules depolymerize. The forces have components parallel to and perpendicular to the anterior-posterior axis. The plus and minus ends of the microtubules are indicated. (B) Mechanical model of the transverse forces (right). It is assumed that there is a process that centers the spindle (to account for the centering at early metaphase); this is represented by the spring. Viscous damping and rearrangements of the cytoskeleton give rise to a positive-damping element, represented by the black dashpot. The motors are represented by a force source (blue) together with a speed-limiting dashpot (blue). The diagonal arrow represents the load dependence of the motors' attached probabilities: the higher the load force, the lower the probability. In the linear circuit (left), the negative-damping and inertial elements (in blue) correspond to the terms in Equations B2 and B3.

Continued on following page

of the damping from the viscosity of the ooplasm [B3] (which might be augmented by the dynamics of the cytoskeleton [B2]). With positive feedback, the swings on either side of the AP axis get larger and larger. This means that any small fluctuation of the position of the pole from the AP axis, as a result of either thermal forces or the finite number of motors, will trigger a sinusoidal oscillation.

To get oscillations that build up in this way, the net damping must be negative (to create positive feedback), but the negative-damping coefficient has to be small in magnitude; otherwise, the pole would move away explosively from the AP axis. The amplitude of oscillation will increase unless either the active components (i.e., the motors) are turned off or the negative damping is opposed by a nonlinear damping term that can cancel the negative damping as the oscillation amplitude increases. Such a nonlinear damping term sets the amplitude of the oscillations in the steady state. A combination of small damping coefficient and a nonlinearity gives rise to a weakly nonlinear oscillator [B4] and results in spontaneous sinusoidal oscillations. This type of oscillator differs from a strongly nonlinear relaxation oscillator, which results in asymmetric sawtooth-shaped oscillations; the model of Joglekar and Hunt for mitotic chromosomes movements [B5], which shares some features such as load-dependent detachment with the present model, is an example of this latter type of oscillator.

The equation of the nonlinear oscillator associated with our model is

$$I\ddot{y} + (\Gamma - \Xi)\dot{y} + \beta\dot{y}^3 + Ky = 0. \quad \text{(B1)}$$

If the damping coefficient is small [$(\Gamma - \Xi)^2 \ll 4IK$], then the equation produces sinusoidal oscillations and the oscillator is termed weakly nonlinear. Note that at threshold $\Gamma = \Xi$, so this condition is automatically satisfied and we expect the oscillations to start out being sinusoidal. K is the stiffness of the centering spring: It produces a restoring force proportional to the position, y, of the pole away from the AP axis. In our model (and see [B1]), K is assumed to be a constant in time and equal on both sides of the embryo. An earlier model [B6] considered the possibility that K differed between anterior and posterior sides, but this was not readily consistent with the spindle-cutting experiments. $\beta\dot{y}^3$ is the nonlinear-damping term: It becomes large when the velocity of the spindle, $\dot{y}$, becomes large. The value of β is a complicated function of the molecular parameters—because its value is poorly constrained, we set β equal to zero in the simulations so that the amplitude of the oscillations is set by the time during which the net damping is negative (i.e., the steady state is not reached). In the cell, we expect that β is likely to be important for setting the maximum amplitude of oscillation, and this will be the subject of later work. Γ is the positive-damping coefficient contributed by the viscosity of the cytoplasm. Ξ is the negative-damping coefficient given by

$$\Xi = 2N\left\{\frac{\bar{f}}{f_c}\bar{p}\left[(1-\bar{p}) - \frac{f_c}{\bar{f}}\right]\right\}f'. \quad \text{(B2)}$$

If it is positive, it gives rise to a force in the same direction as the velocity; it therefore gives rise to "negative damping." I is an inertial term given by

$$I = 2N\left\{\frac{\bar{f}}{f_c}\bar{p}(1-\bar{p})\right\}f'\bar{\tau}. \quad \text{(B3)}$$

I has units of mass and corresponds to a chemomechanical "inertia" because it is associated with a force that is proportional to acceleration ($\ddot{y}$). Note that as expected for an inertial term, $I \approx \Xi\bar{\tau}$, where $\bar{\tau} = (k_{on} + \bar{k}_{off})^{-1}$ is the lag due to the attachment and detachment rates. The numerical value of I is on the order of 100 μg (Figure 5D), nearly three orders of magnitude greater than the actual mass of a one-cell *C. elegans* embryo! This comparison underscores the fact that the present oscillations do not arise from the mass of the cellular structures, as expected because the static and dynamic Reynolds numbers are much smaller than one ([B7], p. 290).

The parameters are as follows. N is the number of motors on each side of the AP axis. $\bar{f}$ is the single-motor force, the load force that is necessary to stall the motor (larger forces are assumed to make the motor go backward [B8]). $\bar{p} = k_{on}(k_{on} + \bar{k}_{off})^{-1}$ is the single-motor activity defined in terms of the attachment and detachment rates as the average fraction of time that the motor spends attached to a microtubule and pulling. Note that the attached probability, p, oscillates about its mean value $\bar{p}$. The detachment rate is assumed to depend on load (f) according to $k_{off}(f) \propto \exp(f/f_c)$, and $\bar{k}_{off} = k_{off}(\bar{f})$ is the off rate at the stall force (about which the motors are assumed to operate).

If the negative damping (Ξ) exceeds a threshold set by the passive damping (Γ) (i.e., $\Xi > \Gamma$), then the total damping becomes negative. In this case, there is positive feedback and the system described by Equation B1 becomes unstable and begins to oscillate. Close to the instability, the angular oscillation frequency measured in radians/s is

$$\omega_0 \approx \sqrt{K/I}. \quad \text{(B4)}$$

If the negative damping falls below the passive damping, then the system is stable and the oscillations die out exponentially.

The oscillation frequency depends inversely on the square root of the inertial coefficient (Equation B4). For fixed k_{on}, I is maximal when $\bar{p}$ = 2/3 (noting that $\bar{\tau} = \bar{p}/k_{on}$), whereas for fixed $\bar{k}_{off}$, it has a maximum when $\bar{p}$ = 1/3 (noting that $\bar{\tau} = (1-\bar{p})/\bar{k}_{off}$). This is

Continued on following page

shown in Figure 5D by the solid and dashed lines, respectively. Because the negative-damping term is near its maximum during the oscillations and $\bar{p} \approx 0.5$ (see Figure 5C), the inertial term is increasing if k_{on} is fixed and decreasing if $\bar{k}_{off}$ is fixed: A decreasing oscillation frequency therefore corresponds to a decreasing $\bar{k}_{off}$.

Box References

B1. Grill, S.W., Kruse, K., and Julicher, F. (2005). Theory of mitotic spindle oscillations. Phys. Rev. Lett. *94*, 108104.

B2. Howard, J. (2006). Elastic and damping forces generated by confined arrays of dynamic microtubules. Phys. Biol. *3*, 54–66.

B3. Alexander, S.P., and Rieder, C.L. (1991). Chromosome motion during attachment to the vertebrate spindle: initial saltatory-like behavior of chromosomes and quantitative analysis of force production by nascent kinetochore fibers. J. Cell Biol. *113*, 805–815.

B4. Strogatz, S.H. (1994). Nonlinear Dynamics and Chaos (Reading, Massachusetts: Perseus Books).

B5. Joglekar, A.P., and Hunt, A.J. (2002). A simple, mechanistic model for directional instability during mitotic chromosome movements. Biophys. J. *83*, 42–58.

B6. Grill, S.W., Gonczy, P., Stelzer, E.H., and Hyman, A.A. (2001). Polarity controls forces governing asymmetric spindle positioning in the Caenorhabditis elegans embryo. Nature *409*, 630–633.

B7. Howard, J. (2001). Mechanics of Motor Proteins and the Cytoskeleton (Sunderland, Massachusetts: Sinauer Associates).

B8. Carter, N.J., and Cross, R.A. (2005). Mechanics of the kinesin step. Nature *435*, 308–312.

The mean frequency of the posterior oscillation was 51.4 ± 8.0 mHz (n = 24 embryos, 23°C), corresponding to a period of 19.6 ± 3.0 s. The oscillation frequency increased with temperature: The slope was +6.3% ± 0.3% per °C (mean ± standard error of the mean [SEM]) between 15°C and 26°C. This is similar to the dependence of the amplitude on temperature (+4.6% ± 1.2% increase per °C).

The sinusoidal waveform suggests that the transverse oscillations arise from a so-called weakly nonlinear oscillator in which the absolute value of the damping coefficient is small compared to the inertial and elastic coefficients [36]. This contrasts with a relaxation oscillator that is strongly nonlinear and has a nonsinusoidal, asymmetric waveform [36] unlike that observed in Figure 1C. Our antagonistic-motors model (Equation B1) is an example of a weakly nonlinear oscillator: At small spindle amplitudes, the individual motors are in what we have termed their force-limited regime [19], meaning that they are operating at low speed and near their maximum force. The transition of a weakly nonlinear oscillator from a nonoscillating to an oscillating mode occurs when the damping coefficient changes sign from positive to negative. In our model, this occurs when the "negative damping" associated with the load dependence of the force generators (Equation B2) exceeds a threshold determined by the positive, viscous damping from the ooplasm. (Negative damping is the opposite of the usual positive damping: As the speed increases, there is an augmenting rather than opposing force.) The threshold can be crossed by changing the number of motors or their activity. By contrast, alternate scenarios such as those in which the activity of the regulatory pathway oscillates do not involve a threshold; reducing the number of motors or their activity would simply reduce the amplitude of the oscillations.

Depletion of Dynein Light Intermediate Chain

In order to obtain evidence for a threshold of motor activity required for oscillations, as predicted by the model, we transferred worms to feeding plates containing bacteria expressing dsRNA directed against *dli-1*, which encodes the essential light intermediate chain of cytoplasmic dynein [29]. With increasing time after transfer, the amount of dynein light intermediate chain decreased as assayed by immunoblotting (see Supplemental Data). At comparatively short times after transfer, 13–16 hr when protein levels were about 50%, the oscillations were either absent or greatly attenuated (Figure 2B; Movie S3; amplitude < 0.25 μm, n = 16/16).

These results are consistent with a recent study [21] showing that oscillations are absent in five of six temperature-sensitive dynein mutants at the permissive temperature, where the total dynein activity is expected to be only partially decreased and other dynein-dependent processes such as spindle centering and posterior displacement were nearly normal. Thus our results as well as complementary results from another laboratory show that partial inactivation or loss of cytoplasmic-dynein function abolishes oscillations, as expected if dynein is an essential component of a force-generating complex whose activity must exceed a threshold for oscillations to occur. At longer times after transfer, the spindles failed to orient properly, a failure that has been found when dynein heavy chain [20] or the dynactin complex [20, 22] is more fully inactivated (Figure 2C, Movie S4).

Depletion of G Protein Regulators Provides Strong Evidence for a Threshold

Because dynein is required for essential processes that precede the oscillations, such as spindle orientation along the AP axis (see above), it is not an ideal protein to deplete in order to investigate the oscillation threshold in detail. We therefore sought additional evidence for a threshold total motor activity by injecting young adult worms with dsRNAs directed against the *gpr-1* and *gpr-2* genes, which encode proteins that regulate the cortical force generators. We confirmed via immunoblotting with anti-GPR antibodies that the levels of the corresponding proteins decreased in a graded manner over 40 hr after injection (Figure 3A, and see Supplemental Data). As the protein levels decreased over time after injection, the severity of the phenotypes increased (Figures 2D–2F, Movies S5–S7). In contrast to the gradual decrease in protein levels, there was a rapid decrease in oscillation amplitude and subsequently a complete loss of oscillation following partial knockdown of *gpr-1/2*.

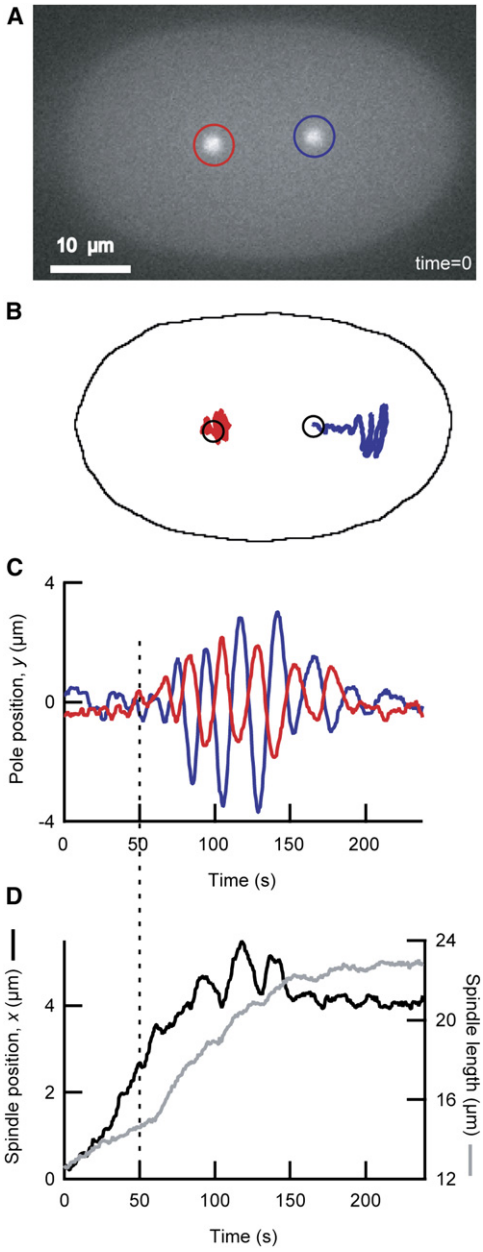

Figure 1. Transverse Oscillations and Posterior Displacement of the Mitotic Spindle in an Unperturbed Embryo

(A) Fluorescence image of the one-cell *C. elegans* embryo showing GFP-tagged γ-tubulin localizing preferentially to the centrosomes (spindle poles). The anterior spindle pole (left) is circled in red, the posterior (right) in blue.

(B) The trajectories of the two poles during metaphase and anaphase measured every 0.5 s. The circles denote the initial positions.

(C) The distances of the spindle poles from the anterior-posterior axis shows the buildup and die-down of the oscillations. The approximate onset of oscillations is indicated by the dashed line.

(D) The position of the spindle (defined as the midpoint of the poles) along the AP axis (black). Zero is the center of the embryo. The slight oscillations are due to the arcing motion of the spindle apparent in the posterior trace in (B). The spindle length is shown in gray. All panels are from the same cell.

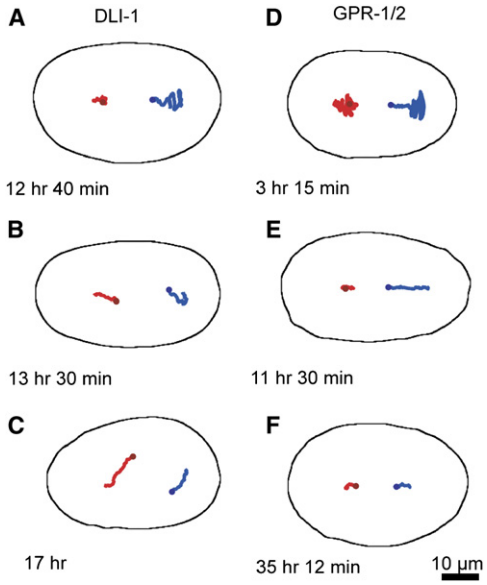

Figure 2. Phenotypes of Progressive Depletion of DLI-1 and GPR-1/2

Examples of the trajectories of the anterior (red) and posterior (blue) spindle poles are superimposed on the contour of the embryo. The circles represent the starting positions. Each panel shows a different embryo.

(A–C) Depletion of dynein light intermediate chain in worms fed bacteria expressing inactivating RNA directed against *dli-1*. (A) An embryo 12 hr 40 min after transfer onto the feeding plates in which the oscillation is normal. (B) A different embryo 13 hr 30 min after transfer in which the oscillation was not present. (C) At 17 hr after transfer, the spindle was not aligned properly on the AP axis.

(D–F) Depletion of GPR-1/2 after injection of dsRNA directed against *gpr-1/2*. (D) At short times after injection, the phenotype is almost normal. (E). At 11 hr 30 min, the oscillations are completely absent, although posterior displacement still occurs. (F) At 35 hr 12 min, there are no oscillations or posterior displacement, although spindles still elongate to 85% of their normal length. Interestingly, all the reduction of spindle elongation occurred over the first 13 hr, suggesting that spindle oscillations may be required to elongate the spindle to its full extent.

The maximum amplitude of oscillations of the posterior pole decreased from ~3 µm to near zero after only 10 hr (Figure 3B), a time at which the GPR-1/2 protein levels had decreased to only 47% (Figure 3A). This strongly supports the existence of a threshold.

Control experiments indicated that at times after injection when the oscillations were lost, there was still sufficient GPR-1/2 protein remaining in the embryo to at least partially activate the force generators. The activity of the force generators was monitored in two ways. First, the force generators generate tension in the spindle. This tension was assessed by cutting the spindle with a UV laser and measuring the initial velocity of the posterior pole toward the posterior side of the cortex [13]. The velocity decreased gradually toward zero as the time after injection increased to 40 hr (Figures 3C). At 9 hr after injection, when the oscillation had all but disappeared (Figure 3B), the initial speed of movement of the posterior pole had decreased only to 60% ± 3% of uninjected controls (SEM, n = 17 embryos assayed between 7 and 11 hr). This shows that the force generators were active, but not at a sufficiently high level to give oscillations, as expected if there is a threshold. The activity of the force generators was monitored in a second way by measuring the total posterior displacement

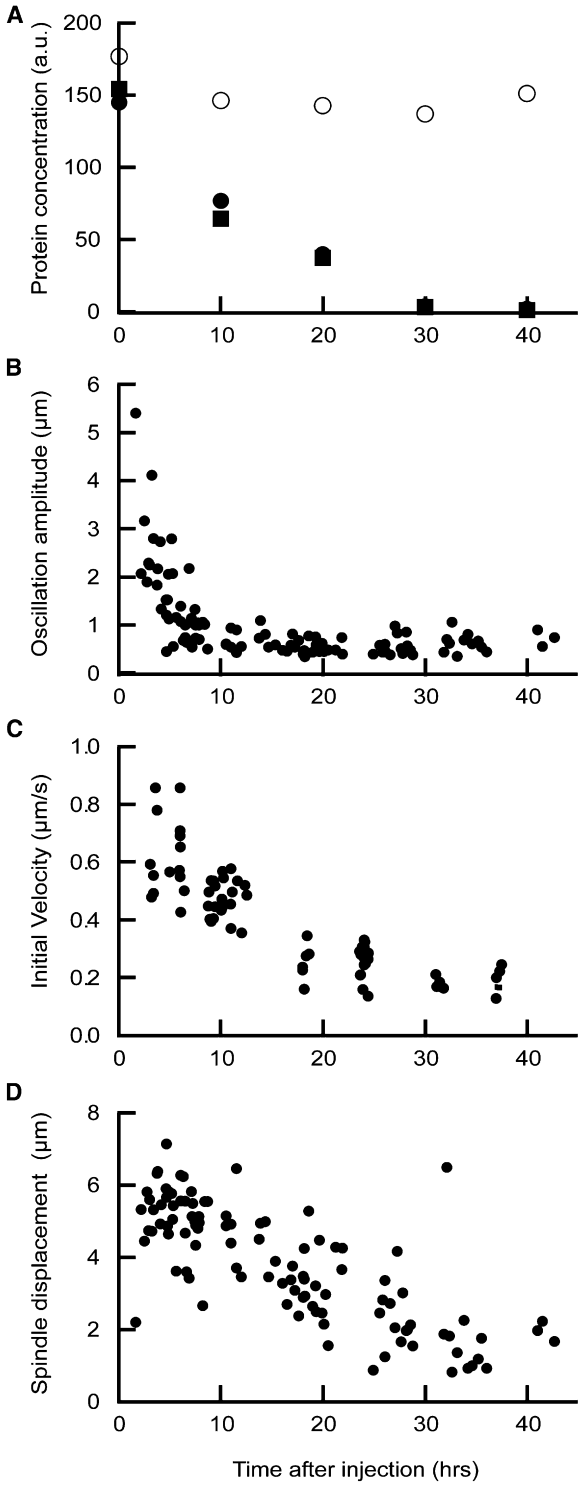

Figure 3. Effect of gradual depletion of GPR-1/2 on spindle movements

(A) As the time between the injection of dsRNA directed against the *gpr-1* and *gpr-2* genes into the mother is increased, the amount of GPR-1/2 protein, assayed by immunoblotting, gradually decreases (● and ■ are two different experiments). The control protein, tubulin (○), doesn't decrease.

(B) The oscillation amplitude decreases sharply after a few hours, falling to near zero at 8 hr after injection. This is consistent with there being a threshold force, as predicted by the model. Each point in panels (B)–(D) indicates a different embryo.

of the spindle pole during metaphase and anaphase in unirradiated embryos. The displacement, which is thought to be driven by the unbalanced tension generated by the cortical force generators [13], decreased gradually toward zero as the time after injection increased to 40 hr (Figures 3D). At 9 hr after injection, the posterior spindle displacement (Figure 3D) had decreased only to 74% ± 5% of uninjected controls (SEM, n = 16 embryos assayed between 7 and 11 hr). Again, this supports the existence of a threshold: Decreasing the activity of the force generators by only one third is sufficient to completely abolish the oscillations.

The Buildup and Die-down of the Oscillations Are Accounted for by a Monotonic Increase in Motor Activity

Having established that a threshold exists, we then asked whether the threshold could also account for the onset and termination of the oscillations. If so, what motor properties might change during metaphase and anaphase to bring the spindle into oscillation and then to bring it out again? According to the model, the oscillations occur because load-dependent motors acting in groups generate negative damping (which produces positive feedback). The negative damping can be increased by increasing the number of motors (N), the activity of the individual motors (defined as the average probability over an oscillation cycle of the motor being attached to the microtubule and generating force, denoted $\bar{p}$), the single-motor force ($\bar{f}$), or other parameters that are associated with the force-dependence of the motors (see Equation B2).

Remarkably, all the qualitative features of the oscillations—the onset, its lag with respect to the spindle displacement (Figures 1C and 1D), and the termination—can all be accounted for by a monotonic increase in the single-motor activity ($\bar{p}$) during metaphase and anaphase. As $\bar{p}$ begins to increase, the spindle begins to move toward the posterior because the total force (and therefore the force imbalance between posterior and anterior sides) is proportional to the single-motor activity. But the oscillations do not begin until the threshold is crossed (when the negative-damping coefficient [Ξ] exceeds the positive-damping coefficient [Γ] in Equation B1). The time required to reach this threshold determines the lag between spindle displacement and oscillation. As the single-motor activity increases further, the negative-damping coefficient actually decreases again (Equation B2) because positive feedback relies on the ability of individual motors to switch between active (attached) and inactive (detached) states. Therefore, as the mean attached probability increases toward unity, switching ceases because the motors are always attached; the negative-damping term then decreases until the net-damping coefficient becomes positive again and the oscillations die down. Thus the oscillations die down even though the mean total force remains high, keeping the spindle in its posterior position. In this way, a monotonic change in a single parameter ($\bar{p}$) can account for

(C) The velocity of the posterior spindle pole, measured just after severing with a UV laser, decreased progressively with time after injection.

(D) Total spindle displacement decreased with time after injection.

the complex choreography of the mitotic spindle during metaphase and anaphase.

The only parameter in our model whose variation can account simultaneously for the buildup and die-down of the oscillations and the steady increase in spindle displacement is the single-motor activity ($\bar{p}$). The negative-damping coefficient depends monotonically on all the other parameters such as the number of motors (N) and the single-motor force ($\bar{f}$), so if these parameters increase steadily during metaphase and anaphase (to account for the steady increase in spindle displacement), then there would be no die-down of the oscillations. If N or $\bar{f}$ first increased (to bring the system into oscillation) and then decreased (to bring it out of oscillation), then the net force (which is proportional to N and $\bar{f}$) would decrease, leading to a reversal of the posterior displacement, which is not seen (Figure 1D). A decrease and then increase in the positive-damping coefficient (Γ) could trigger the buildup and die-down of oscillations but cannot account for the posterior displacement. Similarly, decreasing the centering spring constant (K) could lead to posterior displacement but will not affect oscillations. Thus even in the absence of more complex regulatory mechanisms during the cell cycle, a steady increase in $\bar{p}$ accounts simply for the complex choreography of the spindle during metaphase and anaphase.

The Oscillation Frequency Decreases over the Duration of the Oscillations

We next asked how the single-motor activity, $\bar{p}$, might be regulated during metaphase and anaphase. The attached probability can be increased either by increasing the rate at which the motors attach to the microtubules (increasing the number of pulling motors) or decreasing the rate at which they detach (increasing the time that they pull). In the case of the cortical force generators, an increased attachment rate could correspond to an increase in the rate at which the microtubule binding complex attaches to an incoming microtubule and switches it into a shrinking mode. A decreased detachment rate could correspond to an increase in the time that the complex remains attached to a shrinking microtubule.

The two possibilities can be distinguished. An increase in the attachment rate (k_{on}) over time is predicted to lead to an increasing oscillation frequency, whereas a decrease in the detachment rate ($\bar{k}_{off}$) over time is predicted to lead to a decreasing oscillation frequency. This can be understood by a simple argument because the oscillation frequency reflects the kinetics of association and dissociation of the motors to and from the microtubules: The kinetics become faster when k_{on} increases but slower when $\bar{k}_{off}$ decreases. A more rigorous argument is given in Box 1. To test these predictions, we carefully measured the frequency of the oscillations. The instantaneous frequency was estimated at four times during each period of oscillation (see Figure 4 legend). We found that the frequency of the oscillations decreased over the duration of the oscillations. The frequency decrease was apparent in most embryos, such as that shown in Figure 1. Figure 4 summarizes results from 22 embryos at 23°C: The frequency decreased at a rate of 0.179 ± 0.016 mHz/s (SEM; $p < 10^{-9}$ by Student's t test, n = 22), corresponding to a decrease in frequency of ~40% over the ~120 s duration of the oscillations. Thus we suggest that the steady increase in motor activity during metaphase and anaphase is due to a steady decrease in the detachment rate ($\bar{k}_{off}$).

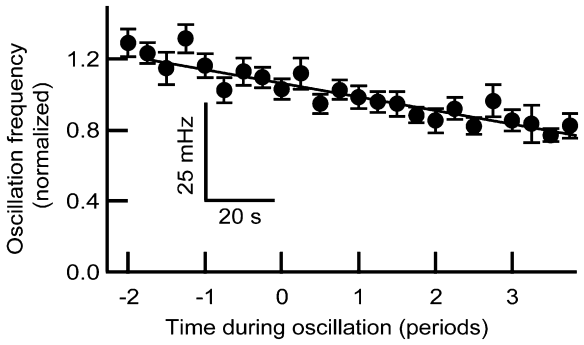

Figure 4. Decrease in Frequency during the Oscillations

The oscillation frequency decreased by about one-third over the duration of the oscillations. Four frequency measurements were made during each period of an oscillation by measuring the times in the cycle at which the position and velocity were at an extremum. The frequency was normalized to that at the peak amplitude and is plotted against time, measured in periods of oscillation, for 22 embryos. The slope is 0.0769 ± 0.0071 (mean ± SEM, $p < 10^{-9}$). The scale bars represent the average oscillation frequency and time for the average oscillation.

Simulation of the Time Course of Spindle Movements

To summarize our findings, we believe that during metaphase and anaphase the motors become more and more processive as a result of a steadily decreasing off rate. As the processivity increases, the motors spend more time attached to microtubules and pulling (i.e., the mean attached probability or single-motor activity, $\bar{p}$, increases), and the net force increases, leading to posterior displacement. When the total motor activity exceeds a threshold, positive feedback due to load-dependent detachment causes the system to become unstable and any spontaneous fluctuations are amplified to produce a buildup of oscillations. However, as the activation of the motors increases further, the ability to switch between active and inactive states diminishes, the system becomes stable again, and the oscillations die down. The simulation in Figure 5 shows that the model accounts for all the qualitative and quantitative aspects of the oscillations: Their onset and decay, the mean frequency, and the decrease in frequency over time (Figure 5E). The expected decrease in the relative oscillation frequency over the duration of the oscillation is 0.064 per oscillation period (Figure 5E and Equation B4), in good agreement with the measured decrease of 0.078 ± 0.07 per oscillation period (Figure 4, legend). The simulation indicates that the oscillations reach their maximal amplitude when the mean attached probability is ~0.5 (horizontal dashed line in Figure 5). The threshold is ~0.25. The same parameters correctly simulate the concurrent posterior displacement of the spindle (Figure 5F).

Discussion

We have shown that an antagonistic-motors model accounts well for the complex dynamics of spindle

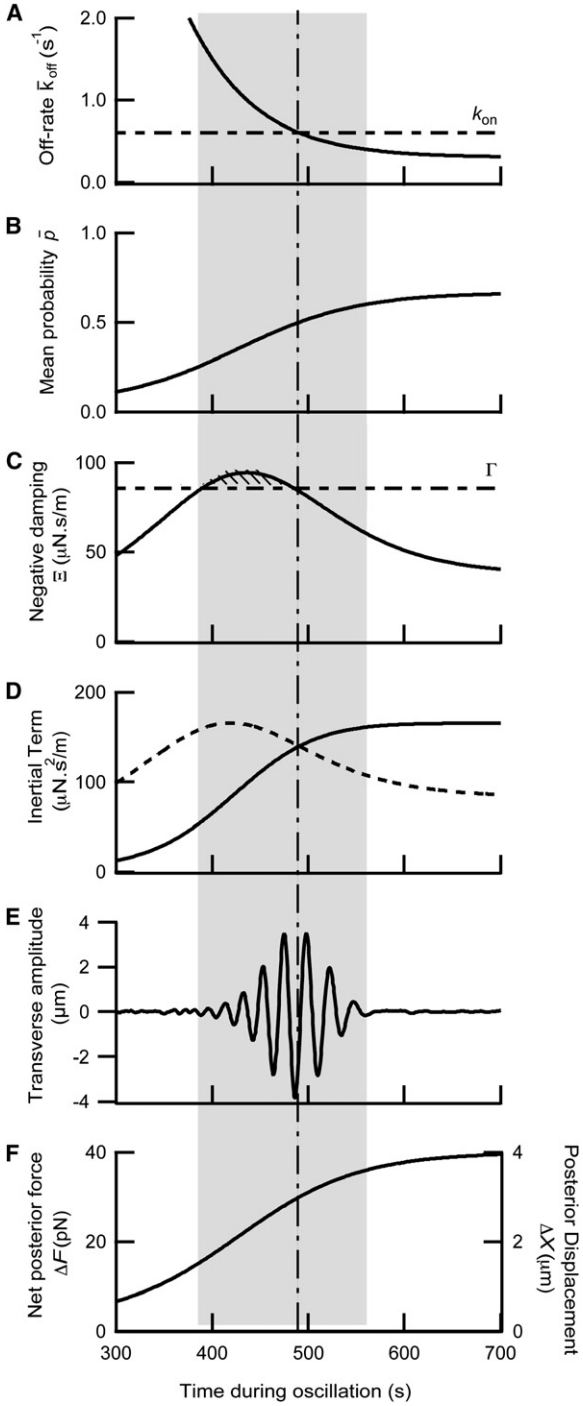

Figure 5. The Antagonistic-Motors Model Accounts for the Buildup and Die-down of the Oscillations

(A) The processivity of the motors is postulated to increase steadily during metaphase and anaphase (i.e., the off rate, $\bar{k}_{off}$, decreases).

(B) As a consequence of the varying off rate, the mean attached probability, $\bar{p}$, a measure of the activity of the motors, steadily increases. The probability is 0.5 when the off rate equals the on rate (k_{on}) indicated by the vertical dashed line in (A).

(C) As the probability increases, the coefficient of negative damping (Ξ) first increases and then decreases. When the coefficient of negative damping exceeds that of the positive damping (Γ), indicated by the horizontal dashed line, the system becomes unstable (shown as the hatched region), and spontaneous oscillations occur. When the coefficient of negative damping drops below the positive damping, the oscillations die out.

(D) The instability occurs while the inertial coefficient (I) is increasing (solid curve). This leads to the observed decrease in the oscillation frequency over the course of the oscillations (Figure 4). The dashed curve shows the case if the on rate were decreasing.

(E) Simulation of the oscillation. The gray region denotes the time when oscillations are resolved above the noise.

(F) Because the probability increases monotonically, so too does the net posterior-directed force and the posterior displacement: Γ = 85.8 μN·s/m, K = 10 μN/m, N = 28, $\bar{f}$ = 6 pN, f_c = 1.5 pN, f' = 3 μN·s/m, k_{on} = 0.6 s^{-1}.

movements during metaphase and anaphase in unperturbed and genetically manipulated embryos.

Evidence for a Threshold Motor Activity Necessary for Transverse Oscillations

The model predicted that there is a threshold of motor activity above which the spindle oscillates and below which it does not. We have confirmed this prediction with two different observations. First, when the activity of the force generators was reduced in a graded manner by reduction in levels of the dynein light intermediate chain or the G protein regulators GPR-1 and GPR-2, the oscillations were abolished even when the protein levels were reduced by only one half. Furthermore, in the case of GPR-1 and GPR-2 inactivation, the abrupt decrease in the amplitude of the oscillations contrasted with the more gradual decrease in both the spindle tension and the posterior displacement, both of which likely reflect the activity of the same motors (see below). And second, we showed that the existence of a threshold can account for the lag between the onset of posterior displacement and the buildup of the oscillations in unperturbed embryos. In addition, we showed that the die-down of oscillations at the end of anaphase can be accounted for by crossing back across the threshold. In summary, graded increases and decreases in motor activity cause abrupt initiation and loss of transverse oscillations, consistent with the existence of a threshold.

Alternative Models for Oscillations

The key idea behind the antagonistic-motors model is that load dependence allows the motor complexes to communicate mechanically from one side of the embryo to the other in order to move the spindle in a coordinated fashion. An alternative is that the motors are activated by regulatory molecules whose activity oscillates through a reaction-diffusion mechanism of the sort that has been postulated to lead to spatio-temporal oscillations in the concentrations of the Min proteins in bacteria [37] and to calcium waves in oocytes and other cells (e.g., [38]). The main argument against such a reaction-diffusion mechanism is that reducing the number of motors is not expected to cause an abrupt cessation of oscillations as observed but rather to a gradual reduction in amplitude. Furthermore, the large size of the *C. elegans* embryo (minor axis is 30 μm) argues against such a reaction-diffusion mechanism. The diffusion coefficient (D) of MinD in protoplasm is 17 $\mu m^2/s$ (K.K., unpublished data) and of buffered calcium in frog ooplasm is 13 $\mu m^2/s$ [39]. With these diffusion coefficients, the estimated time associated with diffusion across the *C. elegans* embryo is ~30 s (time = distance^2/2D), much longer than the time over which the phase of the oscillations changes by one radian (3 s). This makes a reaction-diffusion

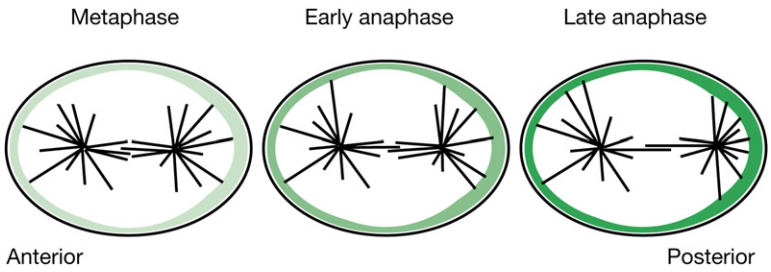

Figure 6. Model of the Time Course of Motor Activation

Prior to metaphase, the pool of motors that can be activated is established at the cortex via GPR-1/2. The size of the pool is indicated by the thickness of the green shaded areas: The pool is larger in the posterior half than in the anterior half but remains constant throughout metaphase and anaphase. Over time, the activity of the motors increases, indicated by the increasing opacity of the green shaded regions. The increasing motor activity accounts for the dynamics of both the oscillations and the posterior displacement.

mechanism unlikely, although a small unbuffered molecule such as IP3 [39] might diffuse fast enough. Likewise, the physical transfer of a chemical signal from one side of the embryo via microtubule dynamics (from cortex to pole on the end of a depolymerizing microtubule and then back to the other cortex on the end of a polymerizing microtubule) would also be too slow, given the microtubule growth and shrinkage rates in the embryo [32]. Because mechanical signaling is fast, it can more rapidly coordinate the activity of molecules over cellular dimensions than can chemical signaling, which relies on the movement of a substance from one side of the cell to the other.

Evidence that One Motor Drives Both Spindle Displacement and Oscillations

By showing that one type of motor can give rise, in a natural way, to very different types of motion—a monotonic displacement along one axis and an oscillation along the other—our findings add significant additional support (over that already mentioned in the Introduction) to the hypothesis that one type of motor underlies the posterior displacement and transverse oscillations. The alternative hypothesis is that different GPR-1/2-regulated motors drive spindle displacement and oscillation and that a threshold of GPR-1/2 activity is required to activate only the oscillation motors. Although we cannot completely rule this out, it does not make sense mechanically: A cortical motor located off the major or minor axis of the embryo will generate a pulling force that has components in both the longitudinal and transverse directions (e.g., starred [*] motor in Box 1, Figure 1), and because of the geometry it is not possible to regulate the two force components independently.

Our RNAi results from dynein light intermediate chain together with analysis of dynein-heavy-chain mutants [21] indicate that cytoplasmic dynein is essential for the transverse oscillations. Therefore, dynein is also expected to be essential for posterior displacement. However, decreasing dynein activity by shifting temperature-sensitive mutants to the restrictive temperature [21] had little effect on posterior displacement, suggesting that posterior displacement is dynein independent. There are two possible explanations for this apparent contradiction. One is that there was only a partial loss of total dynein activity, enough to abolish oscillations (because of the threshold) but not enough to abolish posterior displacement. The other is more subtle. Dynein is necessary for centering the spindle prior to metaphase (e.g., [20]) and could therefore also contribute to the centering stiffness (see Box 1 and [40]); in this case, decreasing the total dynein activity would decrease both the force and the stiffness so that the posterior displacement, which is proportional to the ratio of the two, would be little changed, even if the decrease in dynein is enough to abolish the oscillations.

Relationship between the Current Work and Earlier Work

The current results are in good agreement with earlier results from our laboratory. In the earlier work, the spatial distribution of the force generators was examined at a single time (corresponding to the peak of oscillations) by using a laser to disintegrate the spindle poles [19]. It was found that the force generators were broadly distributed on the cortex. Analysis of the mean and variance of the speeds of the fragments suggested that all the cortical force generators have the same single-motor force ($\bar{f}$), and the variation in fragment speed in each half of the cortex was accounted for by spatial variation in the attached probability (p) but not motor number (N). The posterior cortex had more motors than the anterior one, accounting for the larger net posterior-directed force.

In the present work, we examined how the cortical forces changed over time. We found that the dynamics of the spindle movements were simply accounted for by a monotonic increase in mean motor activity ($\bar{p}$), whereas the motor number (N) and single-motor force ($\bar{f}$) remained constant. This mirrors the earlier results. Indeed, the present results are in quantitative agreement with the earlier ones. Our simulations indicated that the oscillations peak when the mean attached probability of the motors is 0.5 (Figure 5). This is similar to the average probability calculated from the earlier mean-variance analysis: In the posterior half of the cortex, p varied from about 0.25 to 0.75 on opposite sides of the AP axis, giving a mean attached probability ($\bar{p}$) of about 0.5 (Figures 3A and 3C in [19]).

A steady increase in mean motor activity during metaphase and anaphase implies that the total motor activity will increase, in agreement with other laser-ablation studies [14]. According to our analysis, both the number of motors and the single-motor force remain constant, and it is a steady increase in single-motor activity that leads to the increasing force. This is shown in Figure 6.

How Is the Processivity of the Motors Regulated?

In light of our suggestion that the processivity of the motors increases during metaphase and anaphase, it is

interesting that the dynactin complex has been reported to increase the processivity of cytoplasmic dynein [41]. This raises the possibility that the GPR-1/2-dependent activation of the force generators may occur through a dynactin-mediated increase in cytoplasmic-dynein processivity. The link may be LIN-5. LIN-5 associates with GPR-1/2 in vivo and in vitro and is required for both posterior displacement and transverse oscillations [12]. Furthermore, LIN-5 has been suggested, on the basis of functional similarities between GPR-1/2, the vertebrate protein LGN, and the *Drosophila* protein PINS, to be homologous to the vertebrate protein NUMA [42]. Bioinformatic analysis [43] confirms this link by showing that LIN-5 contains an N-terminal calponin-homology domain that is similar to that found in NUMA [44] and may mediate the interaction of the N Terminus of NUMA with the Arp1 subunit of dynactin [45]. Thus there is a potential molecular connection between GPR-1/2 and a motor protein, cytoplasmic dynein; it remains unclear, however, what signal would globally increase motor activity during metaphase and anaphase as indicated in Figure 6.

Role of the Oscillations

We propose that spindle oscillation occurs in the one-cell *C. elegans* embryo because the polarity cues are spatially coarse. The regulation of motor activity is at the level of the anterior and posterior halves of the embryo rather being spatially restricted to the very ends of the embryo. Consequently, force generators on each side of the anterior-posterior axis undergo a tug-of-war. Because it is advantageous for the cell to generate as high as possible force during metaphase and anaphase—higher forces allow the cell to displace the spindle more reliably against external perturbations, and they allow the cell to more rapidly displace the spindle and thus to proceed through mitosis more quickly—the force may exceed the threshold above which spontaneous oscillation is inevitable. Although oscillations are not necessary for asymmetric spindle positioning (the temperature-sensitive dynein mutants are viable at the permissive temperature [21]), they have been a useful tool to probe the internal workings of the mitotic-spindle positioning machinery.

Supplemental Data

Supplemental Data include Experimental Procedures, two figures, and seven movies and are available with this article online at: http://www.current-biology.com/cgi/content/full/16/21/2111/DC1/.

Acknowledgments

The authors thank Mr. H. Bringmann for antibodies to DLI-1; Dr. S. van der Heuvel for antibodies to GPR-1/2; and Drs. C. Cowan, I. Riedel-Kruse, and A. Sanchez and Messrs. H. Bringmann and A. Mashagi for comments on an earlier version of this manuscript. We thank Dr. Bianca Habermann for bioinformatics analysis of LIN-5. J.P. was supported by the Human Frontier Science Program Organization, J.-C.R. by the Studienstiftung des Deutschen Volkes, and S.W.G. by the European Molecular Biology Organization and the Helen Hay Whitney Foundation. A.A.H. acknowledges support from the Deutsche Forschungsgemeinschaft Schwerpunkt Zellpolarität, and J.H. was supported by the National Institutes of Health (AR40593). This work was supported by the Max Planck Society intersectional program the Physics of Biological Systems.

Received: February 10, 2006
Revised: September 5, 2006
Accepted: September 7, 2006
Published: November 6, 2006

References

1. Horvitz, H.R., and Herskowitz, I. (1992). Mechanisms of asymmetric cell division: Two Bs or not two Bs, that is the question. Cell *68*, 237–255.
2. Knoblich, J.A. (2001). Asymmetric cell division during animal development. Nat. Rev. Mol. Cell Biol. *2*, 11–20.
3. Rappaport, R. (1971). Cytokinesis in animal cells. Int. Rev. Cytol. *31*, 169–213.
4. Goldstein, B., and Hird, S.N. (1996). Specification of the anteroposterior axis in Caenorhabditis elegans. Development *122*, 1467–1474.
5. Kemphues, K.J., and Strome, S. (1997). Fertilization and establishment of polarity in the embryo. In The Nematode C. elegans, II, D. Riddle, T. Blumenthal, B. Meyer, and J. Priess, eds. (Cold Spring Harbor, New York: Cold Spring Harbor Press), pp. 335–359.
6. Schneider, S.Q., and Bowerman, B. (2003). Cell polarity and the cytoskeleton in the Caenorhabditis elegans zygote. Annu. Rev. Genet. *37*, 221–249.
7. Cowan, C.R., and Hyman, A.A. (2004). Asymmetric cell division in C. elegans: Cortical polarity and spindle positioning. Annu. Rev. Cell Dev. Biol. *20*, 427–453.
8. Colombo, K., Grill, S.W., Kimple, R.J., Willard, F.S., Siderovski, D.P., and Gonczy, P. (2003). Translation of polarity cues into asymmetric spindle positioning in Caenorhabditis elegans embryos. Science *300*, 1957–1961.
9. Gotta, M., Dong, Y., Peterson, Y.K., Lanier, S.M., and Ahringer, J. (2003). Asymmetrically distributed C. elegans homologs of AGS3/PINS control spindle position in the early embryo. Curr. Biol. *13*, 1029–1037.
10. Tsou, M.F., Hayashi, A., and Rose, L.S. (2003). LET-99 opposes Galpha/GPR signaling to generate asymmetry for spindle positioning in response to PAR and MES-1/SRC-1 signaling. Development *130*, 5717–5730.
11. Gotta, M., and Ahringer, J. (2001). Distinct roles for Galpha and Gbetagamma in regulating spindle position and orientation in Caenorhabditis elegans embryos. Nat. Cell Biol. *3*, 297–300.
12. Srinivasan, D.G., Fisk, R.M., Xu, H., and van den Heuvel, S. (2003). A complex of LIN-5 and GPR proteins regulates G protein signaling and spindle function in C elegans. Genes Dev. *17*, 1225–1239.
13. Grill, S.W., Gonczy, P., Stelzer, E.H., and Hyman, A.A. (2001). Polarity controls forces governing asymmetric spindle positioning in the Caenorhabditis elegans embryo. Nature *409*, 630–633.
14. Labbe, J.C., McCarthy, E.K., and Goldstein, B. (2004). The forces that position a mitotic spindle asymmetrically are tethered until after the time of spindle assembly. J. Cell Biol. *167*, 245–256.
15. Ziegler, H.E. (1896). Untersuchungen über die ersten Entwicklungsvorgänge der Nematoden. Zeitschrift für wissenschaftliche Zoologie. *60*, 351–410.
16. Nigon, V., Guerrier, P., and Monin, H. (1960). L'architecture polaire de l'oeuf et les mouvements des constituants cellulaires au cours des premières étapes du développment chez quelques nématodes. Bull. Biol. Fr. Belg. *94*, 131–202.
17. Dan, K., and Inoue, S. (1987). Studies of unequal cell cleavage in molluscs II. Asymmetric nature of the two asters. Int. J. Invert. Reprod. Develop. *11*, 335–354.
18. Haydar, T.F., Ang, E., Jr., and Rakic, P. (2003). Mitotic spindle rotation and mode of cell division in the developing telencephalon. Proc. Natl. Acad. Sci. USA *100*, 2890–2895.
19. Grill, S.W., Howard, J., Schaffer, E., Stelzer, E.H., and Hyman, A.A. (2003). The distribution of active force generators controls mitotic spindle position. Science *301*, 518–521.
20. Gonczy, P., Pichler, S., Kirkham, M., and Hyman, A.A. (1999). Cytoplasmic dynein is required for distinct aspects of MTOC positioning, including centrosome separation, in the one cell stage Caenorhabditis elegans embryo. J. Cell Biol. *147*, 135–150.

21. Schmidt, D.J., Rose, D.J., Saxton, W.M., and Strome, S. (2005). Functional analysis of cytoplasmic dynein heavy chain in Caenorhabditis elegans with fast-acting temperature-sensitive mutations. Mol. Biol. Cell *16*, 1200–1212.
22. Skop, A.R., and White, J.G. (1998). The dynactin complex is required for cleavage plane specification in early Caenorhabditis elegans embryos. Curr. Biol. *8*, 1110–1116.
23. Hildebrandt, E.R., and Hoyt, M.A. (2000). Mitotic motors in Saccharomyces cerevisiae. Biochim. Biophys. Acta *1496*, 99–116.
24. Lechler, T., and Fuchs, E. (2005). Asymmetric cell divisions promote stratification and differentiation of mammalian skin. Nature *437*, 275–280.
25. Severson, A.F., and Bowerman, B. (2003). Myosin and the PAR proteins polarize microfilament-dependent forces that shape and position mitotic spindles in Caenorhabditis elegans. J. Cell Biol. *161*, 21–26.
26. Etienne-Manneville, S., and Hall, A. (2001). Integrin-mediated activation of Cdc42 controls cell polarity in migrating astrocytes through PKCzeta. Cell *106*, 489–498.
27. Dujardin, D.L., Barnhart, L.E., Stehman, S.A., Gomes, E.R., Gundersen, G.G., and Vallee, R.B. (2003). A role for cytoplasmic dynein and LIS1 in directed cell movement. J. Cell Biol. *163*, 1205–1211.
28. Gomes, E.R., Jani, S., and Gundersen, G.G. (2005). Nuclear movement regulated by Cdc42, MRCK, myosin, and actin flow establishes MTOC polarization in migrating cells. Cell *121*, 451–463.
29. Yoder, J.H., and Han, M. (2001). Cytoplasmic dynein light intermediate chain is required for discrete aspects of mitosis in Caenorhabditis elegans. Mol. Biol. Cell *12*, 2921–2933.
30. Howard, J., and Hyman, A.A. (2003). Dynamics and mechanics of the microtubule plus end. Nature *422*, 753–758.
31. Dogterom, M., Kerssemakers, J.W., Romet-Lemonne, G., and Janson, M.E. (2005). Force generation by dynamic microtubules. Curr. Opin. Cell Biol. *17*, 67–74.
32. Srayko, M., Kaya, A., Stamford, J., and Hyman, A.A. (2005). Identification and characterization of factors required for microtubule growth and nucleation in the early C. elegans embryo. Dev. Cell *9*, 223–236.
33. Grill, S.W., Kruse, K., and Julicher, F. (2005). Theory of mitotic spindle oscillations. Phys. Rev. Lett. *94*, 108104.
34. Schnitzer, M.J., Visscher, K., and Block, S.M. (2000). Force production by single kinesin motors. Nat. Cell Biol. *2*, 718–723.
35. Evans, E. (2001). Probing the relation between force–lifetime–and chemistry in single molecular bonds. Annu. Rev. Biophys. Biomol. Struct. *30*, 105–128.
36. Strogatz, S.H. (1994). Nonlinear Dynamics and Chaos (Reading, Massachusetts: Perseus Books).
37. Howard, M., and Kruse, K. (2005). Cellular organization by self-organization: Mechanisms and models for Min protein dynamics. J. Cell Biol. *168*, 533–536.
38. Lechleiter, J., Girard, S., Peralta, E., and Clapham, D. (1991). Spiral calcium wave propagation and annihilation in Xenopus laevis oocytes. Science *252*, 123–126.
39. Allbritton, N.L., Meyer, T., and Stryer, L. (1992). Range of messenger action of calcium ion and inositol 1,4,5-trisphosphate. Science *258*, 1812–1815.
40. Howard, J. (2006). Elastic and damping forces generated by confined arrays of dynamic microtubules. Phys. Biol *3*, 54–66.
41. King, S.J., and Schroer, T.A. (2000). Dynactin increases the processivity of the cytoplasmic dynein motor. Nat. Cell Biol. *2*, 20–24.
42. Du, Q., and Macara, I.G. (2004). Mammalian Pins is a conformational switch that links NuMA to heterotrimeric G proteins. Cell *119*, 503–516.
43. Bowman, S.K., Neumuller, R.A., Novatchkova, M., Du, Q., and Knoblich, J.A. (2006). The Drosophila NuMA homolog Mud regulates spindle orientation in asymmetric cell division. Dev. Cell *10*, 731–742.
44. Novatchkova, M., and Eisenhaber, F. (2002). A CH domain-containing N terminus in NuMA? Protein Sci. *11*, 2281–2284.
45. Clark, I.B., and Meyer, D.I. (1999). Overexpression of normal and mutant Arp1alpha (centractin) differentially affects microtubule organization during mitosis and interphase. J. Cell Sci. *112*, 3507–3518.